Cement and Concrete Research 38 (2008) 1197–1209

Contents lists available at ScienceDirect

Cement and Concrete Research

journal homepage: http://ees.elsevier.com/CEMCON/default.asp

Design and function of novel superplasticizers for more durable high performance concrete (superplast project)

Yves F. Houst [a,*], Paul Bowen [a], François Perche [a], Annika Kauppi [b,g], Pascal Borget [c,h], Laurent Galmiche [c,i], Jean-François Le Meins [c,j], Françoise Lafuma [c], Robert J. Flatt [d], Irene Schober [d], Phil F.G. Banfill [e], David S. Swift [e,k], Bernt O. Myrvold [f], Berit G. Petersen [f,l], Kåre Reknes [f]

[a] *École polytechnique fédérale de Lausanne (EPFL), Laboratoire de technologie des poudres (LTP), 1015 Lausanne, Switzerland*
[b] *Institute for Surface Chemistry, YKI AB, Box 5607, SE-114 86 Stockholm, Sweden*
[c] *Physico-Chimie des Polymères et des Milieux Dispersés, umr 7615, ESPCI, 10 rue Vauquelin 75231 Paris cedex, France*
[d] *Sika Technology, Tüffenwies 16, 8084 Zürich, Switzerland*
[e] *Heriot-Watt University, School of the Built Environment, Edinburgh, EH14 4AS, UK*
[f] *Borregaard LignoTech, P.O. Box 162, N-1701 Sarpsborg, Norway*
[g] *Skanska Sverige AB, Råsundavägen 2, SE-169 83 Solna, Sweden*
[h] *Université Catholique de Louvain, Unité de chimie des interfaces, Croix du Sud 2/18, B-1348 Louvain-La-Neuve, Belgium*
[i] *École Normale Supérieure de Cachan, PPSM UMR 8531 CNRS, 61, Av. du Président Wilson, 95235 Cachan Cédex, France*
[j] *Laboratoire de Chimie des Polymères Organiques (LCPO), UMR CNRS 5629-ENSCPB, 16 Avenue Pey Berland, 33607 PESSAC Cedex, France*
[k] *Loughborough University, Freeform Construction Laboratory, Leicestershire, LE11 3TU, UK*
[l] *Unicon, Norway*

ARTICLE INFO

Article history:
Received 16 November 2007
Accepted 16 April 2008

Keywords:
Dispersion (A)
Rheology (A)
Adsorption (C)
Admixture (D)
Superplasticizer

ABSTRACT

In this article we shall describe our quest and ultimate success in furthering our understanding of the action of superplasticizers on the rheology of cement and concrete. By specifically producing superplasticizers with varied architectures, we have been able to show the important structural features of the macromolecules that lead to a successful superplasticizer or water reducing agent. Both polycarboxylate and lignosulfonate polymers have been investigated. Using both non-reactive model MgO powders, three different types of cement blends, the adsorption behaviour and the effect on the rheological properties of these two important superplasticizer families have been used to further develop a conceptual model for superplasticizer — cement behaviour. This paper will deal mainly with the conceptual model, the materials and methods used to asses the polymer adsorption behaviour and rheological properties of the systems studied. We shall briefly describe the adsorption of the polymers onto the different surfaces and their influence on surface charge and rheology and the influence of the various ionic species found in cement pore solutions that may influence polymer-cement affinity. The key factors are shown to be the effective adsorbed polymer thickness and the induced surface charge which can be influenced by the polymer architecture, the pore solution composition and the initial particle surface charge.

1. Introduction

In the current study we shall present the final results of a research project carried out within the 5th European Framework Programme. Dispersion of agglomerated cement particles is a key point for improving the workability of concrete or to reduce the amount of mixing water. This is the role of superplasticizers (SPs) or high range water reducers (HRWR In this project called Superplast, we have investigated the structure-function relationship of different superplasticizers (SPs) in concrete leading to: (i) a better understanding of how SPs work and (ii) new tailored SPs ready for exploitation. This has improved our capability to incorporate industrial by-products and recycled concrete within the concrete with large environmental benefits, leading to a more efficient use of the superplasticizers, and better materials compatibility. With a combination of microscopic and macroscopic studies, using state-of-the-art techniques, we have determined the adsorption behaviour, interfacial conformations and interparticle forces together with the rheological properties of model suspensions, 3 cements and fresh concrete mixes. In this paper we describe the conceptual model, the materials and methods, the adsorption of the polycarboxylate and of the lignosulfonates type SPs and in particular their interaction with ions in solution.

The high degree of flexibility for chemical modification of the polycarboxylic-based SPs is used to elucidate the connections between polymer structure and function in detail. It should be stressed that the approach taken in this project is generic and of importance to

* Corresponding author. Tel.: +41 216932848; fax: +41 216933089.
E-mail address: Yves.Houst@epfl.ch (Y.F. Houst).

0008-8846/$ – see front matter © 2008 Elsevier Ltd. All rights reserved.
doi:10.1016/j.cemconres.2008.04.007

technological progress in a broader context since it can be applied to a number of industrial sectors such as coatings, ceramics processing and filled polymers, where the structure-function relationships and tailoring of polymeric additives are of key importance. First, we have produced and selected the polymers, cements and model powders. This also involves the characterisation of all the materials to give a solid base from which to start. Second, a careful characterisation of the interactions between the polymers and the inorganic materials has been performed. This led to a conceptual model describing the influence of the important cement and superplasticizer parameters on the rheological properties of cements and concrete. Third, the knowledge gained in the previous steps was used in the design of tailored superplasticizers for optimal performance in some specific applications. All the polymers have been evaluated in extensive concrete testing.

Two polymer types have been investigated in the project: polycarboxylates and modified lignosulfonates. Four new polymers of each type were specially designed to give as much information as possible regarding the relation between the structure of the polymer and the concrete performance. To conduct the careful analysis that leads to a deeper understanding for the polymer behaviour at the cement grain surfaces we needed a good model system that is a non-reactive "cement". For this, we used dead burnt MgO together with different salt solutions that mimic the pore solution. Based on the knowledge gained from the interaction between model powders and polymers, two new tailored polycarboxylates and one new lignosulfonate polymer were developed. These polymers have been tested in cement and concrete applications to carefully characterise their interactions in real systems. Main results on the concrete testing are described elsewhere [1].

Dispersion of agglomerated cement particles is a key point for improving the workability of concrete or to reduce the amount of mixing water. This is the role of superplasticizers or high range water reducers (HRWR). In this paper we shall start with a brief overview of the role of SPs in cement dispersion providing us with a conceptual model. We will then describe in detail the materials and methods used before discussing the results of the polymer architecture and pore solution on the adsorption and rheological properties of the cements and powder slurries investigated.

2. Conceptual model

2.1. Background

Van der Waals forces play an important role in the properties of numerous materials and in particular with respect to interparticle forces in cement suspensions. The Lifshitz's theory was a major advance and founded our current understanding of these forces [2,3]. In the last fifty years, it was successfully applied to various practical problems involving interparticle interactions [3]. The forces are essentially attractive in suspensions of one type of particle (i.e. the same crystalline phase). The balance between these attractive forces and the repulsive forces due to surface charge or adsorbed species governs the behaviour of particulate suspensions [4]. The DLVO theory takes into consideration the sum of these interparticle forces, and can be used to understand and predict the suspension stability and rheology. This theory has been applied to cementitious systems [5–8] despite the fact that cement suspensions are not really in the colloidal domain. These approaches have proven to be very useful, but the large complexity of such systems was generally not taken fully into consideration, perhaps undermining some of the conclusions that may have been drawn from the approach. In more recent years attempts have been made to take into account the complexity of the ionic medium of cement suspensions, the effects of their broad particle size distributions and their interaction with superplasticizers [6,7]. Steric repulsion, which plays a key role in the action of superplasticizers of the latest generation, can be taken into account by applying de Gennes model [9]. The key parameters, which govern the steric repulsion, i.e. the adsorption layer thickness and its conformation at the solid liquid interface are often difficult to quantify and have been a key issue in the Superplast approach, i.e. how to better measure or estimate this key factor.

The total interaction force can be obtained by taking the sum of the three main interaction forces, i.e. van der Waals or dispersion forces (F_{vdW}), electrostatic (F_{ES}) and steric forces (F_{Ster}). Since all these forces depend linearly on $\bar{a}$ the mean harmonic radius of spherical particles of different sizes a_1 and a_2 [6,8], it is possible to introduce an interparticle force parameter $G(h)$ given by:

$$G(h) \cong (F_{vdW} + F_{ES} + F_{Ster})/\bar{a} \tag{1}$$

h is the separation distance between particle surfaces and $\bar{a} = 2a_1a_2/a_1 + a_2$.

The intergranular friction between particles has been found to be important in the rheology of cementitious systems. The lubrication of contacts by superplasticizers has been recently highlighted [10,11]. However, this parameter has not been considered in the present work.

In general, the attractive forces found in cement suspensions create a rigid network, which prevents the cement from flowing without applying a certain shear force. The magnitude of this force, the yield stress, will depend on the interparticle forces and how these are modified by the presence of an adsorbed layer of superplasticizer. The prediction of rheological properties with respect to interparticle forces for various ceramic systems has, in general, shown very good qualitative agreement but not a quantitative agreement [5,12,13]. Various reasons have been invoked, one being that the interparticle forces are a function of particle size and hence size distribution and most calculations are limited to using some average diameter [5,14,15]. When we consider a stable ceramic suspension, solids loadings towards the maximum packing fraction can be approached (65% volume solids) with the suspension remaining a fluid. For cement suspensions even with superplasticizers attractive non-flowing networks can be formed at much lower volume fractions around 48% solids loading (W/C ratio of 0.35). The reason behind this stress bearing network at low solids fraction, is that the attractive forces between particles form agglomerates that trap a certain amount of the water, which in a stable ceramic suspension can lubricate the flow of ceramic particles past one another. So, a cement suspension is in fact like a cluster of agglomerates, which have a higher effective volume than the real solids volume present. This effective volume has to be decreased by breaking apart a certain fraction of the attractive particulate network in order to allow the cement suspension to flow.

A strategy has been developed to see what decrease in effective volume fraction of solids would be needed so that the attractive cement network can be broken down enough to flow [16,17]. This will be directly related to the number and type of pairs of interacting particles (agglomerates) that can be broken apart by a given shear stress, since the doublets have a larger effective volume than the individual particles because of the liquid trapped between them as illustrated schematically in Fig. 1(a). The dispersion of different doublets with different individual particle sizes will not have the same effect on rheology, as each individual pair will have different effective to real volumes (Fig. 1(b and c)). The amount of volume lost per interacting particle pair, $\Delta V_{k,l}$, can be estimated by various geometries including a truncated cone [16] which is tangent to both spheres as shown in Fig. 1(a). This volume is given for two unequal spheres with radii a_k and a_l by:

$$\Delta V_{k,l} = \frac{2\pi}{3}\,\hat{a}^2(4\hat{a} - \bar{a}) \tag{2}$$

where $\hat{a}$ is $(a_k+a_l)/2$.

Using a particle packing model to create a microstructural picture of the interacting particles [18], which takes into account the particle size distribution, a maximum interparticle force can be calculated according to Eq. (1) [6,8,16,17]. This is illustrated in Fig. 2 for a model

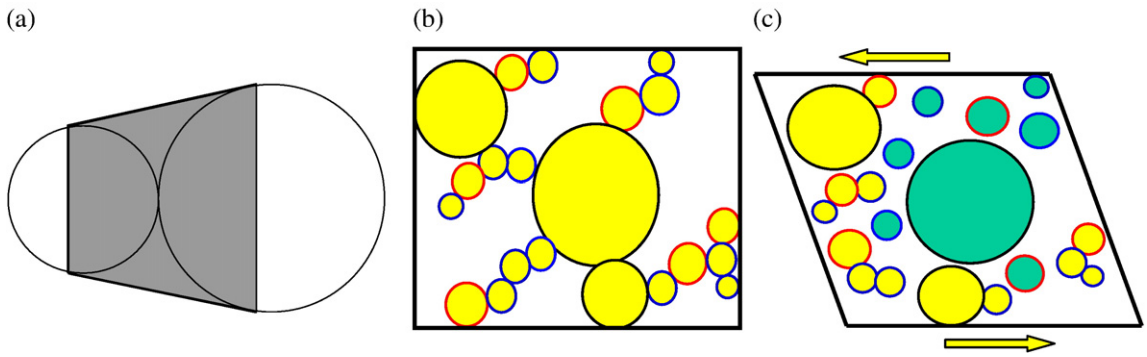

Fig. 1. (a) Truncated cone used to determine the effective volume change due to a doublet (b) different pairs of doublets illustrating the different effective volumes for different pairs (c) illustration showing a certain fraction of "disrupted" pairs at a certain shear stress.

MgO powder with the key parameters being the adsorbed layer thickness and induced surface charge from the superplasticizer adsorption. In the absence of electrostatic repulsion this maximum is reached for separations of about twice the maximum length of the polymer layer extending from the surface into the solvent i.e. the steric effect of the adsorbed polymer alone plays the stabilising role. When electrostatic effects come into play, the point of first repulsion can be beyond this distance. Thus we see in Fig. 2 that the steric effect can be significantly enhanced by electrostatic repulsion, provided the surface potential can be placed at the outer bound of the adsorbed layer [5,7]. These interparticle forces can then be used with the effective volume freed on agglomerate disruption to predict a yield stress for the attractive network as recently proposed in [16].

This model has been used for a cement (Cauldon) with a typical particle size distribution, very close to our model non-reactive MgO powder and other cements used in the Superplast project (see next section Fig. 5). Fig. 3 shows the predicted yield stress for two different surface potentials (0 and −10 mV) as a function of adsorbed layer thickness for this cement. Particle packing modelling was used to find the distribution of nearest neighbour pairs of particles with different sizes [17]. As the particle size distribution is very similar to the model MgO powder and cements investigated, we will be able to compare these predictions with the yield stress measured for the Superplast systems described in the next section.

2.2. Specificity of cement suspensions

Cement suspensions are complex mineral suspensions. Portland cement is composed of roughly five mineralogical phases: alite (impure C_3S), belite (impure β-C_2S), C_3A and C_4AF, and gypsum. These phases may not always be ground to the same fineness when producing cement powder from a clinker. Different size fractions may therefore differ in composition. Cement particles are also often composed of two or more of the above phases which may have different surface properties. Different Portland cements, with similar chemical composition can exhibit different behaviours with respect to the same superplasticizers which may be a consequence of this heterogeneous surface chemistry. Hence, it is often difficult to attribute specific behaviours to specific characteristics of the cements. Furthermore, hydration modifies cement particle surfaces over time. A certain fraction of the superplasticizer can be trapped during hydration in organo-mineral phases (OMP), and is thus no longer available for plasticizing concrete [20]. When cement is contacted with water, numerous ions dissolve and the so-called pore solution becomes far from an ideal electrolyte. The ionic composition of the solution evolves with time and also depends on the cement type [6,19]. The interparticle interaction forces are strongly influenced by the ionic composition of the pore solution. Such difficulties in studying fundamental structure-properties relationships of superplasticizers can partially be overcome by using non-reactive model powders. MgO, which has surface properties at high pH close to that of cement suspensions (low positive charge), has recently been successfully used for adsorption and rheological studies of superplasticizers [21,22].

Steric repulsion, which plays a key role in the action of superplasticizers of the latest generation, can be taken into account by applying the de Gennes model [9]. The key parameters, which govern the steric repulsion, i.e. the adsorption layer thickness and its conformation at the solid liquid interface are often difficult to quantify and have been a key issue in the Superplast approach, i.e. how to better measure or estimate this key factor. According to Fig. 3, the two key parameters are the adsorbed polymer layer thickness and the resulting surface charge. The

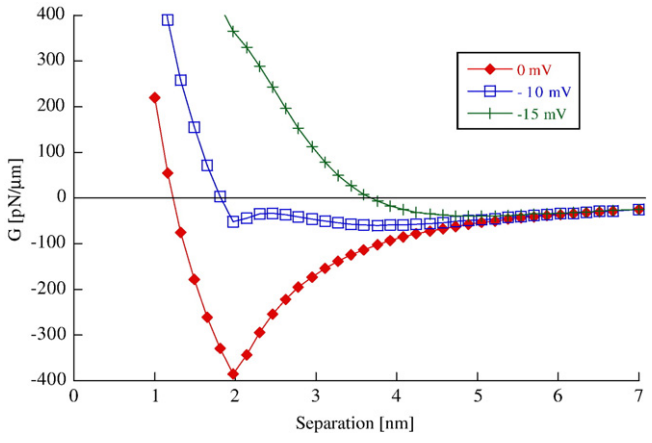

Fig. 2. Normalised interparticle force as a function of particle separation for three potentials. Positive values indicate repulsion and negative values attraction. The adsorbed layer thickness is 1 nm. The normalised force is computed for 1 µm MgO particles in the equivalent symmetric electrolyte representation of a cement suspension [19].

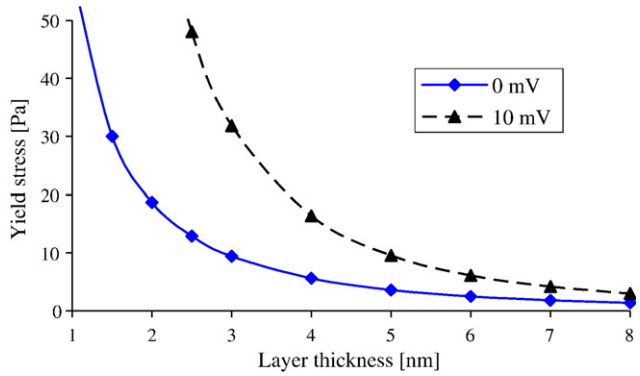

Fig. 3. Yield stress expected for a cement suspension (w/c=0.35) with two different surface potentials.

Table 1
Main parameters used for computing forces and methods used for their evaluation

Parameter	F_{vdW}	F_{ES}	F_{Ster}	Method
Powder particle size distribution and packing arrangement	+	+	+	Direct measurements and distribution model
Hamaker constant of the powder	+			Computation from cement composition
Surface potential with adsorbed SP		+		Zeta potential measurements and potential modelling
Electrolytes in the cement solution (ionic force)	+	+		Measurements and solution modelling
Polymers in solution and adsorbed layer thickness		+	+	AFM and SLS[a] and LS[b] and viscosimetry and modelling

[a] SLS: Static Light Scattering.
[b] DLS: Dynamic Light Scattering.

Table 2
Characteristics of the polycarboxylates

Polymer		PCP-1	PCP-2	PCP-3	PCP-4	PCP-5	PCP-6
Molar mass (g/mol)	M_w	23,000	112,000	25,000	61,000	48,000	32′,500
	M_n	13,000	45,000	18,000	28,000	30,000	16,600
	M_w/M_n	1.8	2.5	1.5	2.2	1.6	2.0
Side chain (M_w) (g/mol)		1000	1000	2000	5000	500 3000 $\frac{PEG_{500}}{PEG_{3000}} = 1.5$	1000
%-mol PEG, τ		25	23	12	13	25	30

adsorbed layers have been modelled by surfaces with full coverage. It is only recently that the issue of estimating the thickness of the adsorbed layer of superplasticizers has really begun to be addressed. This has been stimulated by the observation that polymers with side chains of poly (ethylene oxide) usually induce better dispersion with lower zeta potentials values. As a result, awareness of the importance of steric repulsion has grown. The measurements to estimate the layer thickness have been made predominantly by atomic force microscopy (AFM) [23,24]. Producing both suitable substrates and AFM probes for such studies is one of the main challenges for the successful use of this approach. We met this challenge in the Superplast project by using MgO powders and MgO substrates for the AFM measurements — we could then assess the effects of the different polymers in different ionic media directly using AFM. Also the characterisation of the free polymer in solution for the same ionic media (simulated pore solutions) allows us to make a link between the polymer conformation in solution and when adsorbed onto a surface. The degree of surface coverage and the affinity of the polymer for the surface of the model MgO in different simulated pore solutions (from adsorption isotherms) again allowed us to determine at what dosages to carry out the rheological tests for comparison with the modelling approach described in Section 2.1. The main experimental parameters necessary for evaluation of this conceptual model are summarised in Table 1.

The properties of polymers both intrinsic (such as molar mass, degree of substitution, and distribution of grafted chains) and in solution (such as radius of gyration, degree of dissociation and complexation) are also parameters expected to influence the behaviour of SPs in the highly concentrated cement pore solution. The detailed approach and models used to evaluate these parameters are described in more detail in Section 3.5.

3. Materials and methods

3.1. Polymers

3.1.1. Polycarboxylates

The polycarboxylate polymers (PCP) containing grafted PEO moieties (Fig. 4) were supplied by Sika Technology, Switzerland. The samples were received as aqueous solutions of various polymer contents. Six samples with different chemical structures were provided (Table 2). Part of the polymers were purified by ultrafiltration to eliminate low molar mass compounds (5 kDa for PC-1 and PC-2 and 10 kDa for PC-3 to PC-6) and used for critical experiments, such as the adsorption isotherms and zeta potential measurements.

3.1.2. Lignosulfonates

Lignosulfonates (LS) were from Borregaard Lignotec, Norway. Lignosulfonates are strongly polydispersed materials with a very broad molar mass distribution, and they also contain numerous functional groups: carboxylic acid, phenolic hydroxyl, cathechol, methoxyl, sulfonic acid and various combinations of them (Fig. 5 and Table 3). The first four samples (LS1 to LS4) were selected to cover the “corner stones” of all these parameters. The last one (LS5) was an improvement of LS1. They were produced from soft wood, except for LS3 which was produced from ultrafiltration of a calcium hardwood

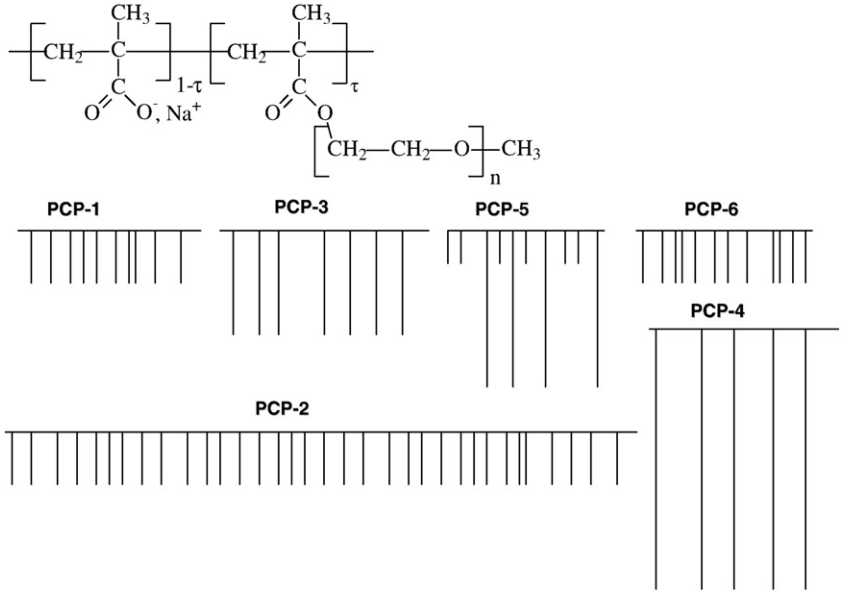

Fig. 4. Schematic illustration of the molecular structure of polycarboxylate polymers.

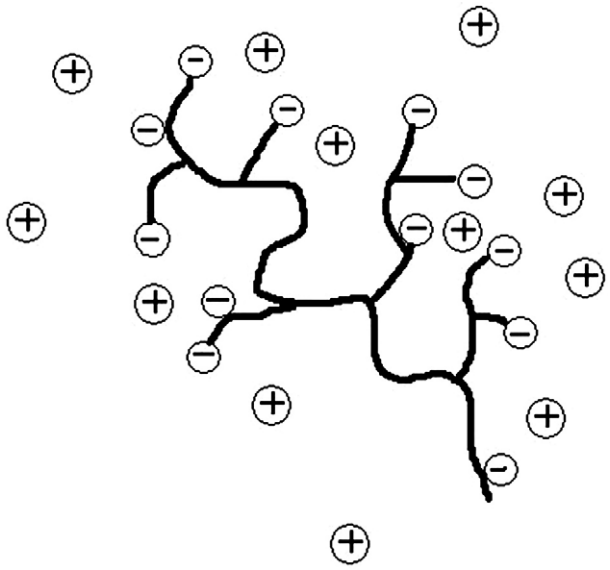

Fig. 5. Schematic illustration of the molecular structure of lignosulfonate polymers.

lignosulfonate. Sugar and impurities were reduced in all samples by ultrafiltration. All samples, except LS4, were spray dried and provided as powders. For characterisation in solution dialysis (5 kDa or 10 kDa membranes) against water was systematically performed. The purification process was followed by centrifugation to eliminate colloidal species in lignosulfonate aqueous solutions.

The softwood lignosulfonates contain predominantly guaiacyl units with one methoxyl group. The hardwood lignosulfonate LS-3 contains both guaiacyl units (with one) and syringyl units with two methoxyl groups. The methoxyl content of LS-3 can thus not be compared directly with the other four.

3.2. Powders and cements

3.2.1. Magnesium oxide

Dead burnt MgO has an isoelectric point of 12.4 [25] and when used together with an electrolyte that has similar ionic composition and pH as cement pore water it has been used successfully as a model system for cement [6,21,22,26,27]. We have found that there is some reactivity of the dead burnt MgO powder [26], where the surface of the powder reacts to form $Mg(OH)_2$. In this project three types of dead burned MgO have been used, referred to as MgO P98, MgO P98C and MgO-R. The difference between P98 and P98C is that P98C was air classified to give particle sizes below 10 μm for electroacoustic measurements. Both powders can be regarded as non-reactive for a period between 30 min and 2 h after first water contact. During this period all surfaces of the MgO grains are expected to have a thin layer of $Mg(OH)_2$. MgO-R is an MgO P98 that has been ground for three hours in a simple rotary ball mill [24] and was produced to give a similar rheology to the reference cement slurry. This milling gave a slightly finer particle size distribution(PSD) particularly in the 30 to 100 μm size range (Fig. 5). All particle size distributions (PSD) were measured using laser diffraction (Malvern Mastersizer, UK).

Table 3
Characteristics of the lignosulfonates

Polymer		LS-1	LS-2	LS-3	LS-4	LS-5
Nature of the wood		Softwood	Softwood	Hardwood	Softwood	Softwood
Counterion		Na^+	Na^+	Ca^{++}	Na^+	Na^+
Molar mass (g/mol)	M_w	86,700	6500	9700	4800	60,200
	M_n	13,050	3050	3300	2300	16,800
Total (organic) sulfur (%)		5.9 (5.8)	6.3 (5.5)	4.5 (4.2)	4.9 (4.3)	5.8 (5.6)
Methoxyl groups (%)		12.1	9.7	11.5	12.6	12.4
Phenolic groups (%)		2.2	2.3	2.0	1.1	2.3
Weak acid groups (%)		3.5	8.0	9.4	5.4	2.7

3.2.2. Micro-cement

Current cements have particles up to about 100 μm in size. Such large particles are not suitable for zeta potential measurements by electroacoustics. A special ultrafine portland cement (UFC) produced by Blue Circle Industries PLC (G.B.) was used. 1% of citric acid was added as a grinding aid. Its particle size distribution was also determined by laser diffraction and is given in Fig. 6. It is similar if not identical to that of the MgO, P98C.

3.3. Cements and cementitious materials

Three selected cements were produced by the dry manufacturing process and are CEM I 42.5 cements. Two of the cements were selected because of their high C_3A (Hope) and low total alkali (Dunbar) contents, characteristics known to affect the performance of superplasticizers in concrete. The third cement from Cauldon was selected as a 'typical' cement. No cement additives, such as water reducing grinding aids, were used during the milling of the three products to avoid added complications when comparing the cements' rheological properties. The cements were also ground on similar cement mills to ensure they had similar particle size gradings and cement paste water demands.

Mainly gypsum was added to Cauldon cement (no anhydrite). In the Hope cement added sulfates were comprised of a mixture of anhydrite and gypsum (40:60 mixture). The Dunbar cement, a low alkali clinker, has a high sulfate content of 1.5–2.0% and a corresponding lower (1.0–1.5%) level of added sulfate (50:50 mixture of anhydrite and gypsum). The main characteristics of these cements are reported in Table 4 and their PSDs are shown in Fig. 7.

3.4. Synthetic "pore solutions"

The influence of ions present in cement suspensions because of hydration reactions, was simulated with the MgO suspensions by addition of various salts. A veritable "soup" of ions which simulates closely a typical pore solution was used for adsorption, electroacoustics and rheology measurements. The compositions of the two

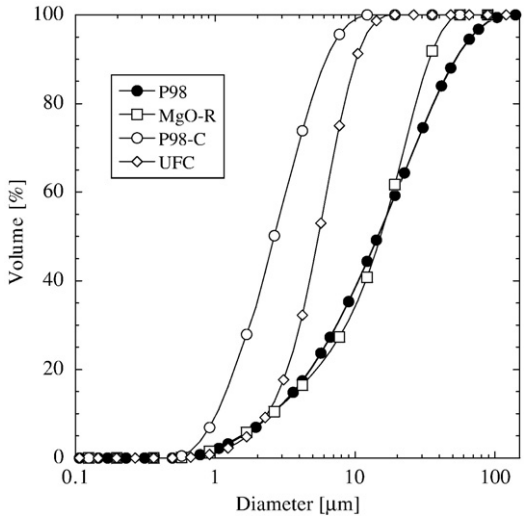

Fig. 6. Particle size distributions of the model MgO Powder (P98), the fine MgO powder P98C and ultrafine cement (UFC) used for electroacoustics and the MgO-R used for the rheology measurements.

Table 4
Main characteristics of the cements

Cement	Hope PC 42.5	Cauldon PC 42.5	Dunbar PC 42.5
SiO_2	20.5	20.7	20.1
Al_2O_3	5.8	4.9	5.2
CaO	64.2	63.6	63.8
SO_3 (total)	3.0	2.9	3.1
Water sol. eq. Na_2O	0.44	0.46	0.36
C_3S	48.5	49.5	53.5
C_2S	22.0	22.0	17.5
C_3A	11.5	8.0	8.0
C_4AF	6.5	9.0	10.5
Hemihydrate+soluble anhydrite [% SO_3]	0.72	1.49	0.78
SSA [m^2/kg]	308	315	313

electrolyte soups used and the resulting pH are given in Table 5 (soup-II was used for rheology experiments because of concerns about possible precipitation but very similar behaviour to soup-I is expected). For the polymer adsorption and electroacoustic measurements, solutions with individual ions were also investigated and they are described and discussed in more detail elsewhere [29–33].

3.5. Polymer characterisation

3.5.1. Molecular structure and phase separation

^1H and ^{13}C NMR spectra were registered in D_2O solutions on a high resolution 400 MHz FT spectrometer. The molar masses are absolute values obtained by triple detection (light scattering, viscosity and refractive index). The molar mass distribution was measured by size exclusion chromatography. The eluent was dihydrogenphosphate 0.1 mol/l at pH 7. The electrical charge was measured by capillary electrophoresis. An automatic capillary viscometer was used to determine intrinsic viscosity in different electrolyte solutions. Conductimetry measurements were also performed to determine the carboxylate and sulfonate group contents in the lignosulfonates.

The cloud point method was used to establish the bimodal demixing curves of PEO in different aqueous salt solutions. Samples were conditioned in test tubes and placed in a transparent thermostated bath. The temperature was slowly increased and the cloud point visually determined. A more detailed presentation of the characterisation methods is given in [34].

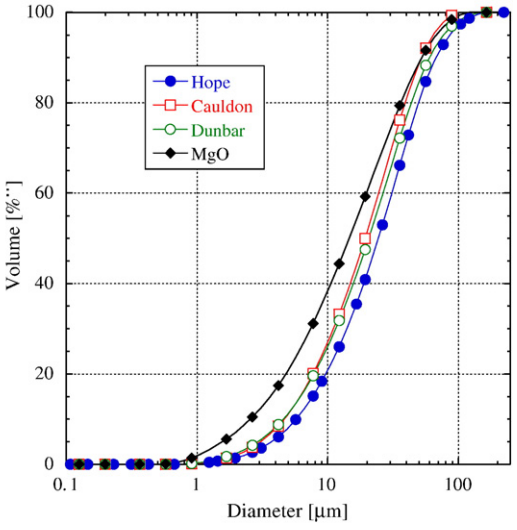

Fig. 7. Particle size distributions of the model MgO Powder (P98) and the three pure cement (Hope, Cauldron, Dunbar).

3.5.2. Conformation in solution

Average radii of gyration and hydrodynamic radii, $\overline{R_g}$ and $\overline{R_h}$, were determined in saline conditions by viscosimetric and light scattering experiments, respectively [34]. Hydrodynamic radii were calculated according to the Stokes law from the diffusion coefficients extrapolated to zero concentration. A Zimm representation was used to extract the average radius of gyration from the angular repartition of the scattered intensity.

3.5.3. Adsorbed layer thickness

The surface force measurements using the colloidal probe technique and the calculations were performed as described in [35] using an MgO surface and an MgO sphere. The aim of these measurements was to get an idea of the polymer conformation on the MgO surface, the polymer layer thickness and help elucidate what mechanisms dominate the dispersion of the powder. The steric forces can be affected by the ionic strength of the solution if it has a strong effect on the conformation of the polymer. Since cement suspensions have a high ionic concentration the force measurements were carried out with the polymer in electrolytes of different ionic strengths. More details can be found in [35].

3.6. Adsorption isotherms

3.6.1. Electroacoustic method

The electroacoustic measurements were used to determine particle size and zeta potential from the dynamic mobility [36]. They also allowed us to study the adsorption of the polymers. An aqueous polymer solution was added by increments with a microburette and the zeta potential was calculated for each increment using Smoluchowsky's model with a correction for the background electrolyte contribution [37]. For measurements, the volume fraction was 2.51% for MgO and 24.1% for cement.

3.6.2. Depletion method

The amount of the adsorbed polymer was measured by the depletion method. A solution of polymer is brought into contact with the powder (solution/powder=0.5 weight fraction) for 30 min. The solid and liquid phases were separated and the amount of polymer in the solution was measured. The difference in the concentration before and after contact with the powder is assumed to be adsorbed polymer. The majority of measurements were carried out in a solution of NaOH 0.01 M (pH 12) and the influence of different ions was studied by adding salts to the solution.

3.7. Rheological measurements

Objective and reproducible rheological testing of cement systems can be hindered by experimental difficulties. In particular, with respect to vertical and centrifugal separation within a rotational rheometer, slippage at the walls of the rheometer, unknown or incompletely controlled mixing energy input (shear history) before or during the test. Recognising these issues, a novel geometry, developed from an earlier helical impeller was designed and used in the

Table 5
Ionic "soups" used to simulate cement pore solutions for adsorption, electroacoustics and rheology measurements

Soup	Mol/l	Ca^{2+}	Na^+	K^+	SO_4^{2-}	OH^-	pH
soup-I	Electroacoustics and adsorption	0.012	0.276	0	0.1	0.1	12.76
soup-II	Rheology	0.0212	0.0978	0.1801	0.0859	0.1486	12.91

The soup-I was prepared with pro analysis NaOH, Na_2SO_4 and $CaSO_4$
The soup-II was prepared with pro analysis KOH, Na_2SO_4 and K_2SO_4 and $Ca(OH)_2$

Table 6
Radii of gyration, hydrodynamic radii and adsorbed layer thicknes (L_{AFM}) for the PCP polymers, (8<pH<12.8 and 0.03<I<0.4 M)

	PCP1	PCP2	PCP3	PCP4	PCP5	PCP6
$\overline{R_g}$ (nm)	5.0±0.7	9.1±0.5	5.2±0.8	7.9±0.4	6.7±0.7	6.2±0.7
$\overline{R_h}$ (nm)	4.9±0.3	10.1±1.0	4.4±0.1	9.3±0.1	5.9±0.3	4.7±0.3
L_{AFM}	1.5±0.5	4.0±1.0	3.5±0.5	4.5±0.5	3.0±1.0	1.5±1.0

SUPERPLAST project [28]. The new geometry was designed to provide the required degree of within-sample mixing, while still enabling both yield stress and plastic viscosity to be determined. The new geometry is an interrupted ribbon helix, which maintains the axial semi profile necessary to permit the well known equations for a concentric cylinder rheometer to be used [28]. The rheometer itself is a CarriMed CSL500 (TA Instruments).

After 30 s hand mixing of the weighed powder and liquid, the paste is poured into the test cup and the test sequence initiated. The paste is subjected to 2 min of stirring at a shear rate of 50 s^{-1}, before the initial test run is carried out. The shear stress is measured at 20 equally spaced shear rate points between 0–10 s^{-1}, followed by another 20 controlled shear rate points from 10–200 s^{-1}. On completion of this initial test sequence the data is automatically saved to file and the paste stirred for a further 5 min at a shear rate of 500 s^{-1}, which is designed to break down any existing structure in the paste. The test sequence is then run again, the data saved to file and the regime terminated. The total time for the whole procedure is approximately 28 min, with the last test run starting at about 20 min, which is consistent with the stability plateau of the MgO powder [26]. The difference between the individual members of the test sets is no more than 2 Pa at a measured level of 100–130 Pa. This is considered to be very good reproducibility of results from separate paste samples. The practical lower limit for the w/c ratio was found to be 0.375. This value of w/c was used for all the tests reported hereafter.

4. Results and discussion

4.1. Polymer characteristics

4.1.1. Polycarboxylates

For all PCPs studied, the ^{13}C NMR results were compared to simulations for a Bernoullian distribution [34] and are in agreement with a random distribution of acids and esters in along the polymer backbone (see Fig. 4).

In cementitious systems, the conformations of the PCPs were expected to be sensitive to pH and to the nature and concentration of salts in the pore solution. Experiments were carried out in the presence of different salts at pH 10 and in the electrolyte soup-I at pH 12.76 which mimics the cement pore interstitial solution. The hydrodynamic radii, $\overline{R_h}$, were, in fact, found to be independent of pH and ionic strength in the range: 8<pH<12.8 and 3×10^{-2}<I<4×10^{-1}. Measurements of the radii of gyration $\overline{R_g}$ via the intrinsic viscosity under similar conditions gave very similar values to the hydrodynamic radii (Table 6).

There is also strong evidence that poly(acrylic acid) and poly (methacrylic acid) form complexes with divalent cations in solution [38–44]. This complexation is regarded to be important for the adsorption of these polymers onto inorganic surfaces. The ratio between COOH groups on the polymer and the amount of divalent cations in solution have been found to be very important for the adsorption onto alumina, and adsorption maxima were found for a [Mg^{2+}]/[acrylic acid monomer] ratio of 0.25 [38] and a [Ca^{2+}]/[acrylic acid monomer] ratio of 0.4 [42]. Foissy et al. [41] also found a phase separation of poly(acrylic acid) in presence of Ca^{2+} at a [Ca^{2+}]/[acrylic acid monomer] ratio of 0.5. However, in our study the presence of the PEO graft chains might influence this complexation process to a large extent. The PEO grafts reduce the rotational freedom of the backbone, making it harder to reach an optimum ratio between COOH groups and cations to form complexes. From the hydrodynamic radii results, neither the ionic strength nor the electrolyte type had any influence on the measured values. This indicates that there is not enough

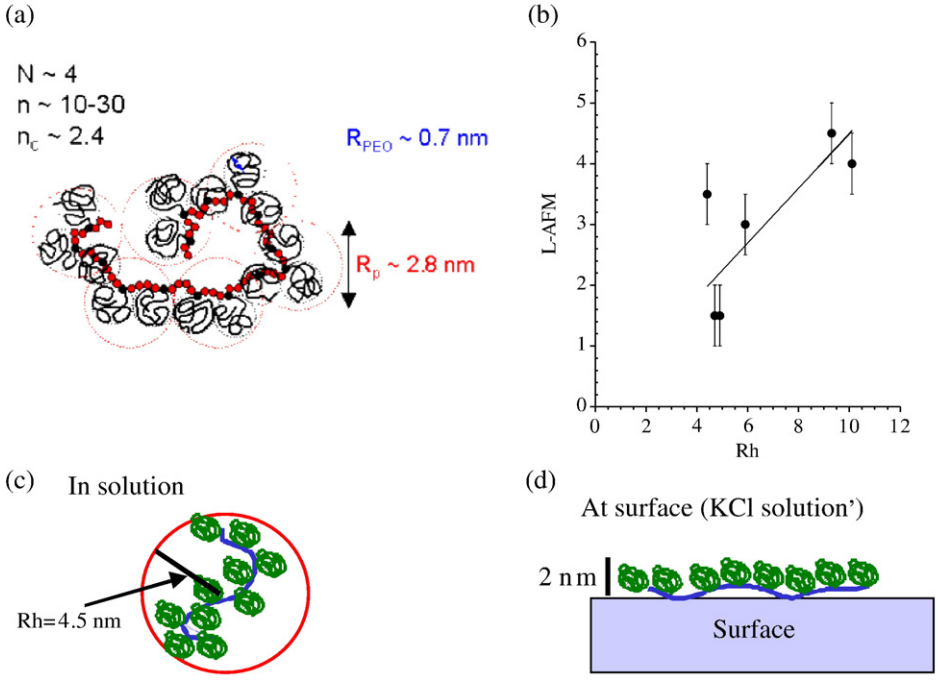

Fig. 8. (a) Model picture of PCP1 found to be in the flexible backbone wormlike regime according to [45], (b) plot of L_{AFM} versus $\overline{R_h}$ showing a roughly linear trend, (c) PC1 conformation in solution according to the hydrodynamic radius and (d) PC1 conformation at surface according to AFM measurements.

Table 7
Calculated radius of gyration from the Flory equation, average molar mass and AFM adsorbed layer thickness (all are averages for ionic strengths from 0.01 to 0.5 M)

	LS1	LS2	LS3	LS4	LS5
$\overline{R_g}$ (nm)	5.2±1.6	1.8±0.6	3.1±1.1	2.0±1.2	4.5±3.0
L_{AFM}	3±1.0	1.5±0.5	1.5±0.5	2±1.0	1.5±0.5

complexation of the COO^- groups in the polymer backbone by the cations in the solution to affect the hydrodynamic radius. However, there may be some complexation, but the strength of the complexes is probably weak compared to the complexes formed with pure poly (methacrylic acid) and therefore they do not change the polymer conformation significantly.

Since electrostatic repulsions are significantly screened under our experimental conditions and accounting for the randomness of the distribution of the grafted PEO chains, the conformations of the polymers were analysed using the model of Gay and Raphaël [45], developed for non-ionic comb-like polymers. In this model, the various possible conformations of a comb homopolymer made of n segments, each containing N monomers along the backbone and P monomers in the side chain are calculated. With these parameters, five different regimes are found. When PCPs were considered within this framework, they were all found to be in the flexible backbone wormlike regime, in which chains are considered to be made of blobs of size D containing n_c segments [34]. An example is given in Fig. 8a where the calculated value of D was found to be 2.8 nm.

The adsorbed layer thicknesses measured by AFM in conditions similar to those for the hydrodynamic radii are also given in Table 6. They are average values from different ionic concentrations to give a general indication of the layer thickness rather than a precise value which is very difficult to achieve under the experimental conditions of high pH and relatively high ionic strength. The general trend is very roughly linear ie as the polymer's $\overline{R_h}$ increases so does the adsorbed layer thickness (Fig. 8b). The adsorbed layer thickness is between 30–75% smaller than the $\overline{R_h}$ (Fig. 8c). From the model picture of the polymer conformation in solution (Fig. 8a) this suggests that the polymer is adsorbed in a roughly linear slightly extended configuration (Fig. 8d). This correlation between the $\overline{R_h}$ ($\overline{R_g}$) and L_{AFM}, thus gives a simple indication of the general trends to be expected. The actual configuration in solution and when adsorbed on the surface of the MgO particles is expected to be more complex than this simple picture. To build up a clearer picture of the relationship between $\overline{R_g}$ and $\overline{R_h}$ and L_{AFM}, a broader family of well characterised polymers is needed.

4.1.2. Lignosulfonates

Studies of lignosulfonate molecules in solution have led researchers to propose that they form either roughly spherical microgels [46] or sheet like structures [47]. The lignin molecule forms polyelectrolyte complexes with many cations [48–52]. In a cement suspension with a high ionic strength and cations such as Ca^{2+} and Al^{3+} present we would thus expect that the lignosulfonate polymers form complexes with these ions. This would make the polymers less soluble in the solution. The high ionic strength of the solution might also decrease the repulsion between adjacent sulfonate groups in the polymer allowing a more coiled conformation in solution akin to the micro-gel model.

The second structural group proposed for lignosulfonates, sheet-like structures, could be formed from branched comb-like polymers. The longest continuous chain would form a "backbone", with shorter branched side chains sticking out. The side-chains might also be further branched, or connect to the backbone again giving closed loops. Since the sulfonation of the lignin molecules breaks an ether bond it is improbable that many sulfonic acid groups are incorporated into the backbone without actually breaking it down to a shorter backbone. Hence, we expect the backbone to be less sulfonated than the side-chains. The conformation of these polymers will be determined mostly by electrostatic forces, pushing nearest charges as far apart as possible.

Both the above models suggest that the $\overline{R_g}$ in solution would be very sensitive to molar mass of the polymer. The adsorbed layer thickness would be expected to be similar to the $\overline{R_g}$ for the microgel case and perhaps lower for the branched comb model. The values of the $\overline{R_g}$ from viscosity measurements and in different electrolytes [53] showed similar values for ionic concentrations between 0.01 and 0.5 M. The average values along with the molar mass and the AFM adsorbed layer thickness measurements are given in Table 7. The relationship of $\overline{R_g}$ with the measured M_w is only approximate but the general trend of increasing $\overline{R_g}$ with M_w is reasonable (Fig. 9a). One of the limitations is that it is difficult to get both accurate M_w and $\overline{R_g}$ values thus the precision of these values is low [54]. The relationship between the adsorbed layer thickness, L_{AFM}, and the $\overline{R_g}$ in solution shows little variation as $\overline{R_g}$ increases (Fig. 9b). Such a trend is also observed with noncharged homopolymers adsorbing in a good solvent [55]. The values of the L_{AFM} are generally lower than the $\overline{R_g}$ by 30–70% suggesting an elongated molecule in solution and an extended flattened adsorption configuration. The AFM colloidal probe measurements thus favour the branched comb or flat sheet model of the lignosulfonate polymers.

The above results show the general trends of the polymers in solution and adsorbed on the surface. The measurements of the radii

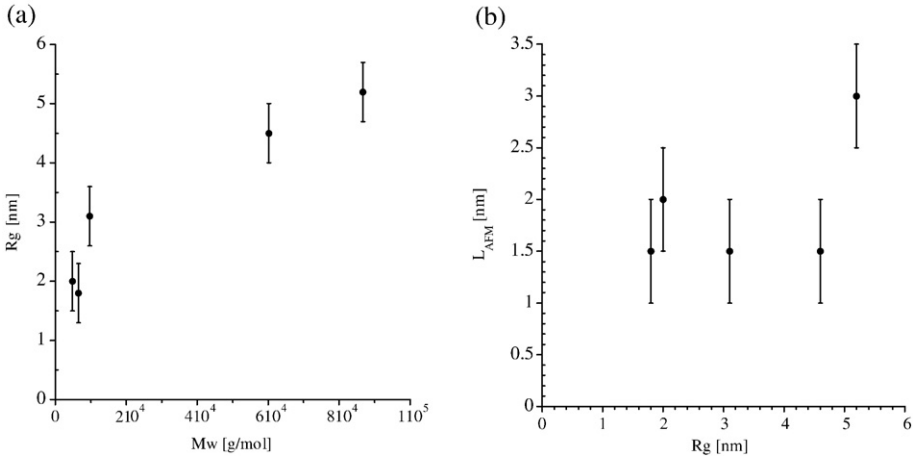

Fig. 9. Plots of radius of gyration, $\overline{R_g}$, versus (a) Molar mass and (b) AFM adsorbed layer thickness for the lignosulfonate polymers.

Table 8
Zeta potential of MgO P98C in different electrolytes

Composition of the solution	Zeta potential [mV]	
	pH 11	pH 13
100 mM NaCl	+3.8	−1.3
100 mM NaCl+10 mM $CaCl_2$	+8	+5
100 mM NaCl+100 mM Na_2SO_4	+0.5	−3

of gyration, hydrodynamic radii and the adsorbed layer thickness all have limitations in the accuracy of measurement. The radii in solution are relatively insensitive to the ionic strength whereas the AFM adsorbed layer thicknesses did show some sensitivity but within the accuracy of the experimental uncertainty. Future work needs to improve the accuracy of these measurements (particularly the AFM) to help us better interpret the adsorbed layer configuration, perhaps on single crystal surfaces for MgO and perhaps pure phase materials for the cement adsorption.

4.2. ζ potential of MgO

The adsorption of the SPs, which are polyelectrolytes with a certain number of dissociated groups, onto MgO is expected to be influenced by the pore solution pH and by the ionic composition of the pore solution. The first point to confirm was the effect of the pH and ionic composition on the surface charge or zeta potential of the model MgO powders. A suspension of MgO P98C containing 0.01 mol/l of KCl was prepared. Its equilibrium pH was 11.1. To this suspension, a NaOH (30%) solution was progressively added by means of a micropipette and the ζ potential was recorded [26]. The isoelectric point (iep) was measured at pH 12.45. It is close to the value commonly given in the literature, i.e. at pH 12.4 [25]. The zeta potential values in presence of different ions are presented in Table 8. As expected from the iep, the surface charge is positive at pH 11 and negative at pH 13. However, when Ca^{2+} ions are added they interact with the MgO powder and the zeta potential increases to more positive values even at pH 13. Sulfate ions also affect the zeta potential but in this case towards a less positive or a more negative value. This shows that both Ca^{2+} and SO_4^{2-} ions interact with the MgO surfaces. However, other experiments have shown that there is no chemisorption of SO_4^{2-} onto the MgO surface [29]. Apparently the interaction between the MgO surface and the SO_4^{2-} ion is not strong enough to chemisorb but is strong enough to affect the zeta potential. The SO_4^{2-} interaction would be expected to affect polymer adsorption as reported for polycarboxylate-type superplasticisers [56]. Recently, a new "hyper-branched" polycarboxylate type polymer showed adsorption behaviour in a 2 mol/l solution of Na_2SO_4 where the amount was found to be almost unaffected by the high SO_4^{2-} concentration. It was thought that this behaviour was due to a higher adsorptive force of the highly structured polymer compared to the SO_4^{2-} ions [57].

4.3. Adsorption of polymers

4.3.1. Adsorption on MgO

The interparticle forces and thus our conceptual model of how SPs act in the dispersion of cement particles assume a constant adsorbed layer thickness. This is expected to be a reasonable assumption if the surface is saturated with adsorbed polymer i.e. at the plateau value for an adsorption isotherm. Therefore adsorption isotherms were made for all polymers at pH≈12 (NaOH 0.01 M). All adsorption curves have the same trend a linear portion followed by a non-linear section ending in a plateau (Figs. 10 and 11) with the exception of PCP3. The linear section indicates that the adsorbed quantity is proportional to the amount of superplasticizer added. The experimental points of this part were fitted linearly by Eq. (3).

$$y = ax \tag{3}$$

The steeper the slope of this linear portion of the isotherm the higher the affinity of the superplasticizer should be for the surface of the powder. Thus we can use the slope a as an indication of this affinity between the SP and the particle surface, the results are shown in Table 9.

The second part of the curve is non-linear and the adsorbed polymer amount increases up to a plateau value. The experimental points of this part of the adsorption curves were fitted by Eq. (4).

$$y = \frac{bcx}{1+cx} \tag{4}$$

b and c are constants. b is the plateau value ($x \to \infty$) and is recorded in Table 9. The plateau values allowed us to estimate the amount of polymer needed for the AFM measurements and the rheological property measurements where we model a fully covered surface with a constant adsorbed layer thickness. Also electroacoustic measurements were made to follow the change in zeta potential as a function of adsorbed polymer. The details of the electroacoustic measurements are presented and discussed in more detail elsewhere [29,30] and only the zeta potential values at the plateau are recorded here for use in the conceptual model (Table 9).

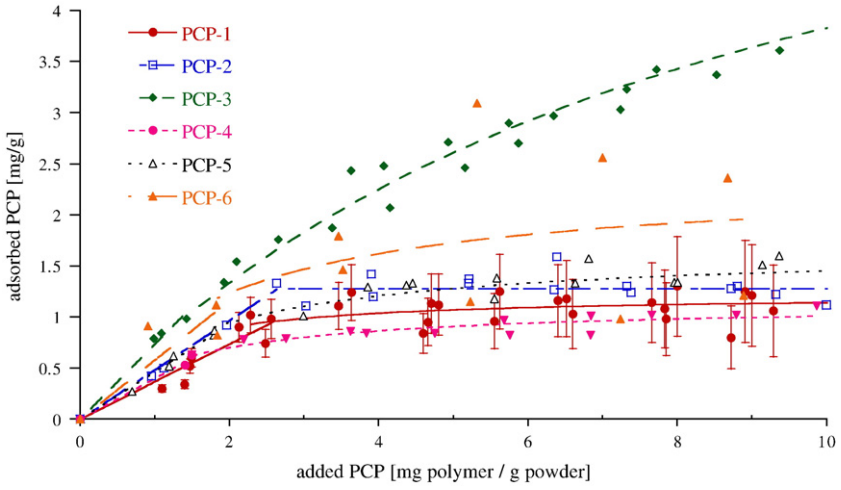

Fig. 10. Adsorption isotherms of PCPs onto MgO P98 in NaOH 0.01 mol/l.

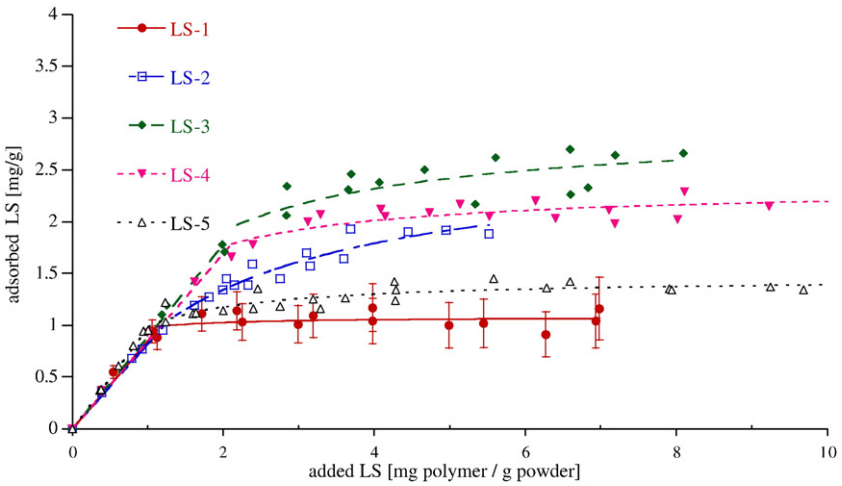

Fig. 11. Adsorption curves of LSs onto MgO P98 in NaOH 0.01 mol/l.

Except for PCP-3, the adsorbed amount increases to a plateau value which varies as a function of the polymer studied. For PCP-1, PCP-2, PCP-4, PCP-5 and PCP-6, all isotherms are similar. For PCP-3 at a concentration higher than 4 mg/g, the adsorbed PCP-3 amount seems to increase almost linearly with the PCP-3 concentration in the supernatant. These results suggest a precipitation of the polymer on the MgO particles or some micellization process which may lead to the removal of the micelles during the filtration step of the measurement method.

The adsorption curves of all lignosulfonates are presented in Fig. 11. As for the PCPs, they can be divided into to two parts: an initial linear response and an asymptotic second part allowing the calculation of a plateau value. Both the slope, *a* (affinity) and plateau values are given in Table 9.

The data in Table 9 show moderate affinities (*a* between 0.4 and 0.6) for all the PCP macromolecules, except for PCP3 which exhibits a different general behaviour. They all induce moderately negative zeta potentials between −2.4 and −8.2 mV. The LSs show a much higher affinity for the MgO and induce significantly higher (negative) potentials between −13.4 and −24.0 mV under the simple test conditions of 0.01 mol/l NaOH. Adsorption isotherms for PCP5 and LS5 made in the ionic "soup-I" showed similar affinities for the surface (0.5 and 0.9 respectively) but higher adsorption plateaus. For the PCP this was above 5 mg/g compared to the 1 mg/g seen in a simple 0.01 M NaOH solution which may indicate some degree of precipitation as seen for PCP3. For the LS5 the effect was less marked going from 1.4 to 1.9 mg/g. A possible reason for the changes in adsorption capacity is the modification of surface charge and ionic concentrations at the near surface, as highlighted in Table 8. In fact for PCP5 and LS5 the induced zeta potential at the plateau of adsorption is reduced when adsorption is made from the ionic "soup-I". For the PCP1 it is reduced form −8.2 to −1.3 mV and in the case of the LS5 from −24.0 to −15.3 mV. The effect of the ionic soup on adsorption and on the decrease in zeta potential values is attributed to the combined effects of charge screening and perhaps complexation [29–31].

The results for the adsorption isotherms of the polymers were used to define the amount of polymer needed to saturate the surface of the powder for the rheological measurements described below in Section 4.4.

4.3.2. Adsorption of SPs on cements

The adsorption of the six polycarboxylate polymers onto the Cauldon cement are described in more detail elsewhere [1]. The adsorption plateau was often difficult to assess because of the hydration reactions taking place and consumption of the SPs by these hydration reactions as generally accepted [20]. Best estimates of adsorption plateaus for the Cauldron cement have been included in Table 9. For the PCPs the values are of the same order of magnitude as the MgO model powder, illustrating the usefulness of MgO as a model "non-reactive" powder. The LS polymers show polymer adsorption or consumption that is an order of magnitude higher than on the MgO powders. The ranking order of the adsorption plateau on MgO and cement follow the same qualitative trends i.e. from highest to lowest adsorbed polymer LS3>LS2>LS4>LS5>LS1. The zeta potentials at the adsorption plateaus were also measured for most polymers on the ultrafine cement (Table 9). The induced potentials are very close to those measured for the MgO model powder and although not identical again confirm the great utility of using MgO as a model powder.

4.4. Rheology

The rheological behaviour of the model MgO-R powder paste and the three different cements without admixtures are shown in Fig. 12. The results from two separate experiments are shown for all three cements — showing the good reproducibility of the new interrupted ribbon helix geometry. All the slurries showed a yield stress. The Hope cement showed the highest and the MgO-R in water showed a similar behaviour to the other two cements (Cauldon and Dunbar). The use of the "soup-II" had a significant effect on the MgO-R rheological behaviour reducing the yield stress by nearly a factor of 2. The reason for

Table 9
Adsorption characteristics for the different SPs on MgO P98 and cements

SP	PCP1	PCP2	PCP3	PCP4	PCP5	PCP6	LS1	LS2	LS3	LS4	LS5
Slope, *a*	0.37	0.48	0.74	0.40	0.47	0.58	0.85	0.82	0.89	0.85	0.98
Plateau value, *b* [mg/g]	1.14	1.28	>2.0	1.01	1.45	1.99	1.07	2.24	2.66	2.2	1.39
ζ [mV] plateau	−8.2	−6.8	−5.0	−2.4	−4.5	−7.0	−18.4	−17.7	−17.4	−13.4	−24.0
Cauldron plat. [mg/g]	1.45	1.95	>2.0	1.5	>2.0	1.22	7.9	>50	>50	10.5	8.95
Ultrafine cem. ζ [mV]	−6.1	−6.6	−7.1	−4.8	–	–	−14.7	−13.1	−20.6	−9.6	–

ζ potential measured on MgO P98C from 0.01 mol/l NaOH solutions.

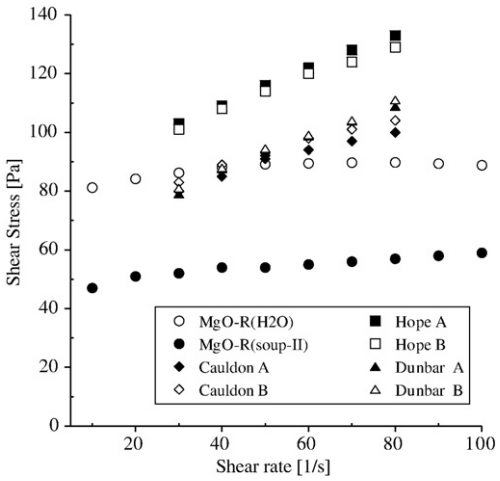

Fig. 12. Rheological behaviour of Model MgO-R powder and cements (Aand B represent repetitions of the same experimental conditions for the cements).

this behaviour remains unclear for the moment but is probably related to a modification of the surface charge for different ionic solution conditions as shown in Table 8. Scrutiny of the rheological data shows that the pastes under study were producing a consistent linear relationship between shear rate and shear stress in the shear rate region of 30–80 s^{-1}. A linear regression analysis of the results for this region in each case provides intercept and slope data which are proportional to yield stress and viscosity respectively. Comparison of the intercept values is therefore a good indication of the effect of any given variable on the rheology of the system under study.

The effect of four PCPs on model MgO-R powder paste rheology, as indicated by the intercepts is illustrated in Fig. 13 for two different dosages. The 0.17% dosage corresponds to the adsorption plateau for these polymers (except for PCP3). The 1% dosage was closer to the values often used in practice because of a certain amount of consumption [20] in cementitious systems. All the PCP polymers, at the dosage levels studied, have a marked effect in reducing the intercept value of the studied pastes, with polymer PCP2 giving the best results. The use of the electrolyte soup-II as the gauging liquid slightly lessens the effectiveness of the polymers, with the exception of PCP2. This polymer has the highest molar mass, and lowest side chain length.

The effect of four LS polymers on the model MgO powder paste rheology, as indicated by the intercept values is illustrated in Fig. 14. All the polymers, at the dosages tested, lower the intercept values dramatically, with LS2 giving the best result. The use of the electrolyte soup as the gauging liquid leads to a slight decrease in the effect, with the exception of pastes containing LS2, where there is no observable effect. The LS2 polymer has the lowest molar mass, the lowest % of methoxyl groups but the highest phenolic OH, calcium and sulfate levels. The complexity of the LS2 chemistry does not allow us to make a clear conclusion on why LS2 behaves differently.

When we compare the rheological behaviour of the MgO powder and the pure cement phases with the results from the model shown in Fig. 3 we see that the behaviour is well described. All the polymers induce a negative charge on the surface of the fine cement and the fine MgO between −1 and −15 mV (Table 9). Without any adsorbed

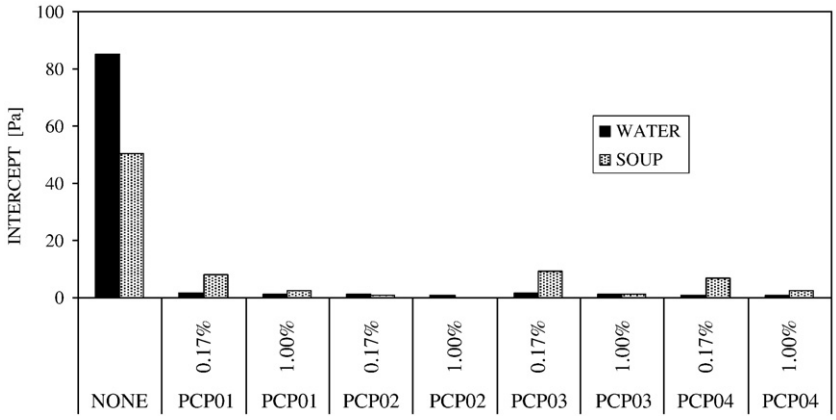

Fig. 13. Effect of polycarboxylate polymers on MgO paste intercept value (uncertainties on measured values are±3 Pa).

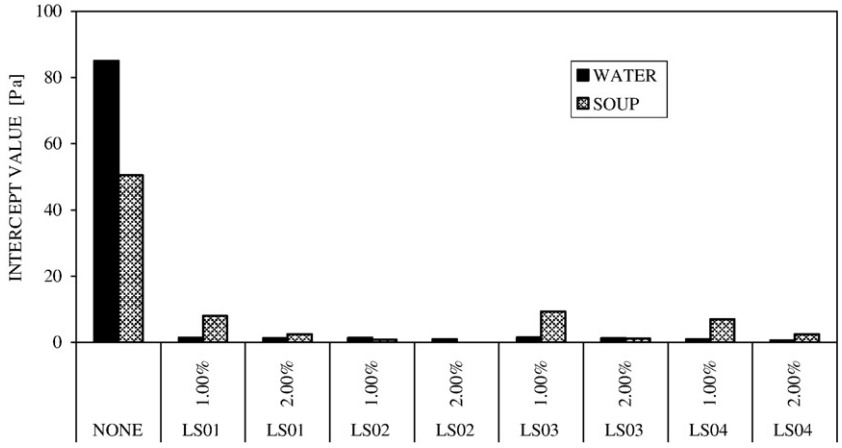

Fig. 14. Effect of lignosulfonate admixtures on MgO paste intercept value. (Uncertainties on measured values are±3 Pa).

polymer the yield stresses are predicted to be greater than 50 Pa (Fig. 3) showing a good correspondence with the measured results for both the model MgO powder P98 (50 to 80 Pa) and the pure cement phases (70 to 90 Pa). The model then predicts a significant drop in the yield stress to lower than 10 Pa, for surface charges of around −10 mV and layer thickness greater than 2 nm. This was also observed in the rheological measurements where yield stresses dropped to between 1 and 10 Pa for the various polymers. This is in very good agreement with the AFM data where the polymers were shown to have an effective adsorbed layer thickness of between 1.5 and 4.5 nm. From the effect of the ionic "soup" on the amount of adsorbed SP and induced zeta potential described in Section 4.3 above we saw a reduction in zeta potential and an increase in adsorbed amount. This suggests that although the layer thickness is slightly higher the possible change of zeta potential reduces the effectiveness of the SPs. These results are consistent with the conceptual model predictions shown in Fig. 3 where a reduced zeta potential would increase the yield stress for the adsorbed layer thicknesses measured for these systems. These results show that the model predicts the effect of superplasticizer and cement suspension yield stress very well, at least semi-quantitatively.

The rheological testing on the pure cement phases more or less mirrored the results on the MgO. All PCPs reduced the yield stress to below 1 Pa (except for the combination of Hope and PCP 1 which was still low at around 10 Pa). For the LSs the yield stresses were again lowered to between 5 and 10 Pa for the Hope and Cauldron cements and even lower with the Dunbar cement. Again all the results fit qualitatively into the conceptual model results shown in Fig. 3. To take the predictive capacity towards a more quantitative level, more accurate determination of the adsorbed layer thickness and the ionic structure of the near surface layers are needed. Also studies with a broader family of SP molecules will help to see how generic the approach is. The rheological testing of the cements and concretes with fly-ash and silica fume are discussed in more detail elsewhere [1] and show a more complex behaviour.

5. Conclusions

The results we have show the great practical potential of the yield stress model (YODEL) when used in combination with careful characterisation of the polymer or superplasticizer (SP) architecture both free in solution or adsorbed onto a particle surface. The use of a combination of methods to characterise the effect of the adsorbed polymer (AFM colloidal probe measurements, electroacoustics and adsorption isotherms) as well as slurry properties (rheological measurements) give an excellent overview of polymer behaviour at the cement-grain interface.

MgO was again shown to be a very good model powder for the evaluation of a superplasticizer's influence on surface potentials and rheological properties. This was especially true for the polycarboxylates where we get very similar adsorption and induced zeta potential plateaus for MgO and cement. For the lignosulfonate macromolecules, polymer consumption is an order of magnitude higher for cements but the zeta potential induced on MgO is very representative of cementitious systems. The MgO has also allowed us to demonstrate the effects of isolated ions on the solid-polymer interaction but further work is still needed here to see how such insights are transferable to cement systems. The conceptual model of a polymer's interaction with a powder surface, used in conjunction with a quantitative yield stress model, was successful in describing the rheological properties of the cement slurries with different polymers and confirmed by rheology measurements on the model MgO slurries.

The polymer conformation in solution, as suggested by the radius of gyration, R_g and hydrodynamic radius, R_h, was shown to be similar to that of the adsorbed layer thickness measured by atomic force microscopy. For the polycarboxylate polymers (PCPs) the AFM measurements show an adsorbed layer thickness about half of the R_g and R_h values measured in solution indicating the molecules are flattened in their adsorbed state. For the PCPs this is to some degree expected, as although the particle surface is charged its surface potential is low in magnitude and should be able to accommodate a flattened rather than brush-like conformation. For the lignosulfonates the situation was less clear and although the AFM adsorbed layer thickness was often lower than the R_g. This may suggest that the macromolecules studied have a more branched comb-like structure than a spherical microgel structure.

The use of a simulated pore solution to mimic the different ionic species in cement pore solutions affects both the surface charge of our model powder and the adsorption of the polymer. This in turn modifies the rheological behaviour. The effects on the model powder surface potentials are small and thus it is difficult to ascertain the exact role of the different species and or mixtures of species in the proximity of the particle surface.

All these insights should allow us to suggest modified polymer structures and test their conformation in simulated pore solutions to provide better dispersion and compatibility with different pore solution compositions before testing on cements. The knowledge gained allows a qualitative approach to the design of efficient macromolecules but there is still a need for deeper understanding of the near surface interfacial zone (<4 nm) where a high ionic concentration is expected. The composition and structure of this near surface layer may influence the binding of the polymer to the particle surface. One approach to investigate this in more detail would be to use single crystal surfaces, such as MgO or calcite that are chemically stable or at least kinetically stable within the time frame of AFM measurements. Work with substrates of pure cement phases would also be enlightening if the surfaces were kinetically stable for such experiments.

The future goal for this type of modelling approach is to evaluate in a more quantitative manner the yield stresses and rheological behaviour for multi-component mixtures. This may be achieved for both the model powders such as MgO with alumina and silica, and the cements with industrial by-products such as fly-ash, silica fume or slag. Despite having been developed for cementitious materials, the model is generic and can be applied to other systems of industrial or environmental importance, whose particle size domain is different, such as ceramics, chocolate, waste slurries and soils.

Acknowledgments

This work was carried out within the 5th European Framework Programme (Contract G5RD-CT-2001-00435) and received a financial support from the Swiss Federal Office for Education and Science (contract No 00.0273-1).

References

[1] P.F.G. Banfill, P. Bowen, R.J. Flatt, L. Galmiche, Y.F. Houst, A. Kauppi, F. Lafuma, P. Livesey, U. Mäder, B.O. Myrvold, F. Perche, B.G. Petersen, K. Reknes, I. Schober, D.S. Swift, Improved superplasticisers for high performance concrete: the SUPERPLAST project, 12th International Congress on the Chemistry of Cement, Montreal, 2007.
[2] R.G. Horn, Surface forces and their action in ceramic materials, J. Am. Ceram. Soc. 73 (1990) 1117–1135.
[3] W.B. Russel, D. Saville, W.R. Schowalter, Colloidal dispersions, Cambridge University Press, 1991.
[4] D.F. Evans, H. Wennerström, The Colloidal domain where physics, chemistry, biology, and technology meet, 2nd ed.Wiley-VCH, New York, etc, 1999.
[5] J.A. Lewis, H. Matsuyama, G. Kirby, S. Morissette, J.F. Young, Polyelectrolyte effects on the rheological properties of concentrated cement suspensions, J. Am. Ceram. Soc. 83 (2000) 1905–1913.
[6] R.J. Flatt, Polymeric dispersants in concrete, in: V.A. Hackley, P. Somasundaran, J.A. Lewis (Eds.), Polymers in Particulate Systems: Properties and Applications, Marcel Dekker, New York, 2002, pp. 247–294.
[7] R.J. Flatt, Y.F. Houst, P. Bowen, H. Hofmann, Electrosteric repulsion induced by superplasticizers between cement particles: an overlooked mechanism ? in: V.M. Malhotra (Ed.), 6th CANMET/ACI International Conference on Superplasticizers and other Chemical Admixtures in Concrete, SP, vol. 195, American Concrete Institute, Farmington Hills, Mi, USA, 2000, pp. 29–42.

[8] R.J. Flatt, Dispersions forces in cement suspensions, Cem. Concr. Res. 34 (2004) 399–408.
[9] P.G. de Gennes, Polymers at an interface: a simplified view, Adv. Colloid Interface Sci. 27 (1987) 189–209.
[10] H. Van Damme, S. Mansoutre, P. Colombet, C. Lesaffre, D. Picart, Pastes: lubricated and cohesive granular media, C. R. Phys. 3 (2002) 229–238.
[11] D. Lootens, P. Hebraud, E. Lecolier, H. Van Damme, Gelation, shear-thinning and shear-thickening in cement slurries, Oil Gas Sci. Technol. — Rev. IFP 59 (2004) 31–40.
[12] L. Bergström, C.H. Schilling, I.A. Aksay, Consolidation behavior of flocculated alumina suspension, J. Am. Ceram. Soc. 75 (1992) 3305–3314.
[13] G.V. Franks, Z. Zhou, N.J. Duin, D.V. Boger, Effect of interparticle forces on shear thickening of oxide suspensions, J. Rheol. 44 (2000) 759–779.
[14] P.C. Kapur, P.J. Scales, D.V. Boger, T.W. Healy, Yield stress of suspensions loaded with size distributed particles, AIChE J. 43 (1997) 1171–1179.
[15] Z. Zhou, M.J. Solomon, P. Scales, D.V. Boger, The yield stress of concentrated flocculated suspensions of size distributed particles, J. Rheol. 43 (1999) 651–671.
[16] R.J. Flatt, P. Bowen, Yodel: a yield stress model for suspensions, J. Am. Ceram. Soc. 89 (2006) 1244–1256.
[17] R.J. Flatt, P. Bowen, Yield stress of multimodal powder suspensions, an extension of the YODEL (Yield stress mODEL), J. Am. Ceram. Soc. 90 (2007) 1038–1044.
[18] P. Navi, C. Pignat, Three — dimensional characterization of the pore structure of a simulated cement paste, Cem. Concr. Res. 29 (1999) 507–514.
[19] R.J. Flatt, P. Bowen, Electrostatic repulsion between particles in cement suspensions: validity of linearized Poisson–Boltzmann equation for non-ideal electrolytes, Cem. Concr. Res. 33 (2002) 781–791.
[20] R.J. Flatt, Y.F. Houst, A simplified view on chemical effects perturbing the action of superplasticizers, Cem. Concr. Res. 31 (2001) 1169–1176.
[21] R.J. Flatt, Y.F. Houst, P. Bowen, H. Hofmann, J. Widmer, U. Sulser, U. Mäder, T.A. Bürge, Interaction of superplasticizers with model powders in a highly alkaline medium, in: V.M. Malhotra (Ed.), 5th CANMET/ACI International Conference on Superplasticizers and other Chemical Admixtures in Concrete, SP, vol. 173, American Concrete Institute, Farmington Hills, Mi, USA, 1997, pp. 743–762.
[22] R.J. Flatt, Y.F. Houst, P. Bowen, H. Hofmann, J. Widmer, U. Sulser, U. Mäder, T.A. Bürge, Effect of superplasticizers in highly alkaline model suspensions containing silica fume, in: V.M. Malhotra (Ed.), 6th CANMET/ACI International Conference on Fly-Ash, Silica Fume, Slag and Natural Pozzolans in Concrete, SP 178, vol. 2, American Concrete Institute, Farmington Hills, Mi, USA, 1998, pp. 911–930.
[23] K. Yoshioka, E. Sakai, M. Daimon, Role of steric hindrance in the performance of superplasticizers in concrete, J. Am. Ceram. Soc. 80 (1997) 2667–2671.
[24] H. Uchikawa, S. Hanehara, D. Sawaki, The role of steric repulsive force in the dispersion of cement particles in fresh paste prepared with organic admixtures, Cem. Concr. Res. 27 (1997) 37–50.
[25] G.A. Parks, The isoelectric points of solid oxides, solid hydroxides and aqueous hydroxo complex systems, Chem. Rev. 65 (1965) 177–198.
[26] R.J. Flatt, P. Bowen, A. Siebold, Y.F. Houst, Cement model powder for superplasticizer properties studies, Proceedings of the 11th International Congress on the Chemistry of Cement, Durban, 2003, 2, Tech Book International, New Dehli, India, 2003, pp. 23–32.
[27] R.J. Gustafsson, K. Reknes, Adsorption and dispersing properties of lignosulfonates in model suspensions and cement paste, in: V.M. Malhotra (Ed.), 6th CANMET/ACI International Conference on Superplasticizers and other Chemical Admixtures in Concrete, SP, vol. 195, American Concrete Institute, Farmington Hills, Mi, USA, 2000, pp. 181–193.
[28] D.S. Swift, P.F.G. Banfill, Effect of superplasticizers, powder fineness, and solution electrolyte content on the rheology of model paste systems, in: V.M. Malhotra (Ed.), 7th CANMET/ACI International Conference on Superplasticizers and Other Chemical Admixtures in Concrete, SP, vol. 217, ACI International, Farmington Hills, Mi, U.S.A, 2003, pp. 499–512.
[29] F. Perche. Adsorption de polycarboxylates et de lignosulfonates sur poudre modèle et ciments, Thèse EPFL No 3041, Lausanne, 2004. (Can be downloaded from http://library.epfl.ch/en/theses/?nr=3041).
[30] F. Perche, Y.F. Houst, P. Bowen, H. Hofmann, Adsorption of lignosulfonates and polycarboxylates — depletion and electroacoustic methods, Proceedings 7th CANMET/ACI International Conference on Superplasticizers and Other Chemical Admixtures in Concrete, Berlin, Germany, 2003, pp. 1–15, Supplementary papers.
[31] Y.F. Houst, P. Bowen, F. Perche, Adsorption of superplasticizers on a model powder, 12th International Congress on the Chemistry of Cement, Montreal, 2007.
[32] B.O. Myrvold, J. Gustafsson, K. Reknes, Adsorption studies of lignosulphonates on cement and cement model compounds, 11th International Congress on the Chemistry of Cement, Durban, 2003.
[33] B.O. Myrvold, Interaction between lignosulphonates and clinker minerals and the hydration products of clinker minerals, 12th International Congress on the Chemistry of Cement, Montreal, 2007.
[34] P. Borget, L. Galmiche, J.-F. Le Meins, F. Lafuma, Microstructural characterisation and behaviour in different salt solutions of sodium polymethacrylate-g-PEO comb copolymers, Colloids Surf. A: Physicochem. Eng. Asp. 260 (2005) 173–182.
[35] A. Kauppi, K.M. Andersson, L. Bergström, Probing the effect of superplasticizer adsorption on the surface forces using the colloidal probe AFM technique, Cem. Concr. Res. 35 (2005) 133–140.
[36] R.W. O'Brien, Electroacoustic effects in a dilute suspension of spherical particles, J. Fluid Mech. 190 (1988) 71–86.
[37] R.J. Hunter, Measuring zeta potential in concentrated industrial slurries, Colloids Surf. 195 (2001) 205–214.
[38] J. Sun, L. Bergström, L. Gao, Effect of magnesium ions on the adsorption of poly (acrylic acid) onto alumina, J. Am. Ceram. Soc. 84 (2001) 2710–2712.
[39] K. Vermöhlen, H. Lewandowski, H.-D. Narres, M.J. Schwuger, Adsorption of polyelectrolytes onto oxides — the influence of ionic strength, molar mass and Ca^{2+} ions, Colloids Surf. A 163 (2000) 45–53.
[40] A. Foissy, A. El Attar, J.M. Lamarche, Adsorption of polyacrylic acid on titanium dioxide, J. Colloid Interface Sci. 96 (1983) 275–287.
[41] C. Geffroy, A. Foissy, J. Persello, B. Cabane, Surface complexation of calcite by carboxylates in water, J. Colloid Interface Sci. 211 (1999) 45–53.
[42] L. Dupont, A. Foissy, R. Mercier, B. Mottet, Effect of calcium ions on the adsorption of polyacrylic acid onto alumina, J. Colloid Interface Sci. 161 (1993) 455–464.
[43] M.A.V. Axelos, M.M. Mestdagh, J. Francois, Phase diagrams of aqueous solutions of polycarboxylates in the presence of divalent cations, Macromolecules 27 (1994) 6594–6602.
[44] S. Iida, Interactions of calcium ions and polyelectrolytes, Biophys. Chem. 57 (1996) 133–142.
[45] C. Gay, E. Raphaël, Comb-like polymers inside nanoscale pores, Adv. Colloid Interface Sci. 94 (2001) 229–236.
[46] A. Rezanowich, D.A.I. Goring, Polyelectrolyte expansion of a lignin sulfonate microgel, J. Colloid Sci. 15 (1960) 452–471.
[47] P. Luner, U. Kempf, Properties of lignin monolayers at the air-water interface, Tappi J. 53 (1970) 2069–2076.
[48] K. Roberts, L. Davidsson, Precipitation of sodium caseinate with dextran sulfates, sodium-dodecyl sulfate, sodium-dodecyl sulfonate and lignin sulfonate, in: M. Kerker (Ed.), Interface and Colloid Science, vol. V, Academic Press, New York, etc, 1977, p. 295.
[49] G. Ström, P. Barla, P. Stenius, Formation of lignin sulfonate-polyethylenimine complexes and its influence on pulp drainage, Sven. Papp.Tidn. 82 (1979) 408–413.
[50] G. Ström, P. Stenius, Formation of complexes, colloids and precipitates in aqueous mixtures of lignin sulphonate and some cationic polymers, Colloids Surf. 2 (1981) 357–371.
[51] G.E. Fredheim, B.E. Christensen, Polyelectrolyte complexes: interactions between lignosulfonate and chitosan, Biomacromolecules 4 (2003) 232–239.
[52] F.E. Brauns, D.A. Brauns, The chemistry of lignin, Academic Press, New York, 1960, p. 178, Supplement volume.
[53] B.O. Myrvold, The polyelectrolyte behaviour of randomly branched lignosulfonates polyelectrolyte, TAPPI J. 6 (2007) 10–14.
[54] G.E. Fredheim, S.M. Braaten, B.E. Christensen, Molecular weight determination of lignosulfonates by size-exclusion chromatography and multi-angle light scattering, J. Chromatogr. A942 (2002) 191–199.
[55] Ref.[4], p. 392.
[56] K. Yamada, S. Ogawa, S. Hanehara, Controling the adsorption and dispersion force of polycarboxylates-type superplasticizer by sulphate ion concentration in aqueous phase, Cem. Concr. Res. 31 (2001) 375–383.
[57] H. Hamada, T. Hamai, M. Shimoda, M. Shonaka, T. Takahashi, Development of new superplasticizer providing ultimate workability, in: V.M. Malhotra (Ed.), 8th CANMET/ACI International Conference on Superplasticizers and other Chemical Admixtures in Concrete, SP, vol. 239, American Concrete Institute, Farmington Hills, Mi, USA, 2006, pp. 31–49.